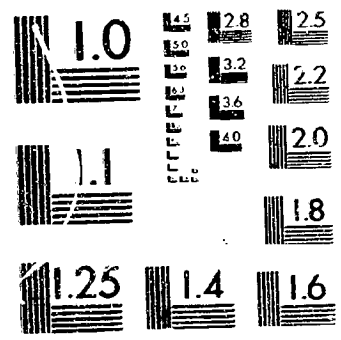


(NA
USI
(SY
HC

1041

-26621

UNCLAS



MICROCOPY RESOLUTION TEST CHART
NATIONAL BUREAU OF STANDARDS 1963-A

NASA Contractor Report 159277

(NASA-CR-159277) TRANSITION PREDICTION
USING THREE DIMENSIONAL STABILITY ANALYSIS
(Systems and Applied Sciences Corp.) 31 p
HC A03/BF A01 CSCL 20D

M80-26621

Unclas
G3/34 23643

TRANSITION PREDICTION USING
THREE DIMENSIONAL STABILITY
ANALYSIS

Mujeeb R. Malik

SYSTEMS AND APPLIED SCIENCES CORPORATION
Hampton, Virginia 23666

NASA Contract NAS1-15604
June 1980



National Aeronautics and
Space Administration

Langley Research Center
Hampton, Virginia 23665



TABLE OF CONTENTS

	<u>PAGE</u>
ABSTRACT	i
NOMENCLATURE	ii
SECTION 1 - INTRODUCTION	1-1
SECTION 2 - WAVE PROPAGATION IN BOUNDARY LAYERS.	2-1
SECTION 3 - NUMERICAL METHOD	3-1
SECTION 4 - RESULTS.	4-1
SECTION 5 - CONCLUSIONS.	5-1
REFERENCES	6-1
FIGURE CAPTIONS.	7-1

ABSTRACT

Several methods of transition prediction by linear stability analysis are compared. The spectral stability analysis code SALLY is used to analyze flows over laminar flow control wings. It is shown that transition prediction by the envelope method and a new modified wave packet method are comparable in reliability but that the envelope method is more efficient computationally.

NOMENCLATURE

A	maximum disturbance amplitude
a_n	Chebyshev coefficients
c	wing chord
f	dimensional frequency
\vec{k}	wave number vector
L	algebraic mapping parameter
N	N-factor = $\ln A/A_0$
R	displacement thickness Reynolds number, $U_x \delta^*/\nu_\infty$
Re_c	chord Reynolds number, $U_\infty c/\nu_\infty$
s	arc length along an arbitrary path on the wing
T_n	Chebyshev polynomial
t	time
U	unperturbed x-velocity in the boundary layer
\vec{U}_p	potential flow vector at edge of boundary layer
U_x	x-component of \vec{U}_p
U_∞	incoming free stream velocity
\vec{V}_g	group velocity vector
v'	perturbation velocity in the y-direction
W	unperturbed z-velocity in the boundary layer
w	mapped coordinate normal to wing surface
x	coordinate in the direction of the normal chord
y	coordinate normal to the wing surface
z	coordinate along the wing span

α	x-wave number
α_A	angle of attack
β	z-wave number
ω	frequency (complex)
Ω	frequency (real)
δ^*	displacement thickness
λ	wave length
ν	kinematic viscosity
θ	wing sweep angle
ψ	angle formed by the wave number vector with the x-axis
ψ_g	angle formed by the group velocity vector with the x-axis
ψ_p	angle formed by the potential flow vector with the x-axis
ϕ	eigenfunction; defined in Eq. (3).
η	adjoint of the eigenfunction

SECTION 1 - INTRODUCTION

In this report several methods of transition prediction using linear stability analysis are compared. The incompressible linear stability computer code SALLY is used in various ways to study three-dimensional boundary layer flow over laminar flow control (LFC) wings. Here we compare the so called envelope method¹ with wave-packet methods², to predict transition. We conclude that the envelope method is at least as reliable as the more complicated and less efficient wave packet method.

Consider the stability of three dimensional laminar flow over swept wings with sweep angle θ . The coordinate system used on the wing is depicted in Fig. 1. The x-axis is in the direction of the normal chord, the y-axis is normal to the surface of the wing while the z-axis is along its span.

Neglecting the curvature of the wing surface, compressibility effects, and non-parallel flow effects, linear disturbances satisfy the Orr-Sommerfeld equation

$$\begin{aligned} & \left(\frac{d^2}{dy^2} - \alpha^2 - \beta^2 \right)^2 \phi \\ &= iR \left\{ (\alpha U + \beta W - \omega) \left[\frac{d^2}{dy^2} - \alpha^2 - \beta^2 \right] \phi - \left(\alpha \frac{d^2 U}{dy^2} + \beta \frac{d^2 W}{dy^2} \right) \phi \right\} \quad (1) \end{aligned}$$

with the boundary conditions

$$\phi(0) = \frac{d\phi}{dy}(0) = 0; \quad \phi(\infty) \text{ bounded.} \quad (2)$$

Here the perturbation velocity in the y-direction is assumed to be of the form

$$v' = \operatorname{Re}[\phi(y)e^{i(\alpha x + \beta z - \omega t)}], \quad (3)$$

$U(y)$ and $W(y)$ are the (unperturbed) laminar boundary layer velocities in the x- and z-directions, respectively, and R is the Reynolds number. It is assumed that all variables are non-dimensionalized with boundary layer scaling.

Equations (1) - (3) constitute an eigenvalue problem for the frequency ω and wavenumbers α, β . For given Reynolds number R , this eigenvalue problem provides a complex dispersion relation of the form

$$\omega = \omega(\alpha, \beta) \quad (4)$$

relating the complex parameters α, β and ω .

Semi-empirical methods to predict transition on LFC wings are based on tracing the evolution of modes across the wing. An appropriate N-factor for transition correlation is defined as the (logarithm of the) total growth factor across the wing (see below). A good transition predictor is one for which transition occurs at nearly constant N for a wide variety of wings and flow conditions.

For natural transition, disturbances of all frequencies are present on the wing surface. In this case, there are many optional ways to compute N factors. The first choice is between temporal and spatial stability theory. In temporal theory, α and β are real while ω is complex; the mode grows in time if $\text{Im}(\omega) > 0$, but the mode does not grow in space. An N-factor for transition correlation may be defined as

$$N = \int_{s_0}^s \text{Im}(\omega) / |\text{Re}(\vec{v}_g)| ds \quad (5)$$

where $\vec{v}_g = (\partial\omega/\partial\alpha, \partial\omega/\partial\beta)$ is the (complex) group velocity and s is the arclength along an appropriate curve on the wing. The N-factor (5) is not fully defined until a prescription is given for singling out a specific mode at each position on the wing and for defining a specific curve on which to integrate. We shall return to these questions in Sec. 2.

In spatial stability theory, ω is real but α and/or β may be complex. Again, there is arbitrariness in the definition of an appropriate N-factor because of the variety of excitable modes on the wing.

WAVE PROPAGATION IN BOUNDARY LAYERS

The complex eigenvalue relation (4) provides two real relations among the three complex quantities α, β , and ω . In temporal stability theory, the requirements that α and β be real provide two more conditions so there remain two arbitrary parameters among $\text{Re}(\alpha)$, $\text{Re}(\beta)$, $\text{Re}(\omega)$, and $\text{Im}(\omega)$.

There are several ways to remove this arbitrariness in the computation of the growth factors N . In the envelope method¹, $\text{Im}(\omega)$ is maximized with respect to α at fixed $\text{Re } \omega$ [which then determines α, β and ω uniquely at each point on the wing] and the curve in (5) is defined to be everywhere tangent to $\text{Re}(\vec{v}_g)$.

With spatial stability theory, there remain three independent real parameters among α, β and $\text{Re}(\omega)$ once the eigenvalue condition (4) is satisfied. One possibility is to require that the direction of most rapid growth, which is parallel to the vector $(-\text{Im}(\alpha), -\text{Im}(\beta))$, be parallel to $\text{Re}(\vec{v}_g)$ and that the resulting value of the most rapid growth rate be maximized with respect to the remaining two independent parameters.³

Alternatively, it is possible to use wave

packet theory to remove the arbitrariness in the definition of N-factors. For a conservative dynamical system, kinematic wave theory implies that a wave packet propagates in physical and wavevector space according to the Hamilton-Jacobi equations⁴

$$\frac{dx}{dt} = \frac{\partial \omega}{\partial \alpha} \quad (6)$$

$$\frac{dz}{dt} = \frac{\partial \omega}{\partial \beta} \quad (7)$$

$$\frac{d\alpha}{dt} = -\frac{\partial \omega}{\partial x} \quad (8)$$

$$\frac{d\beta}{dt} = -\frac{\partial \omega}{\partial z} \quad (9)$$

Nayfeh² considered the extension of Eqs. (6)-(9) to non-conservative systems where α, β , and ω can be complex. Then, ω_α and ω_β may also be complex. For a physical solution with real x, z , and t to exist, (6) and (7) imply that the group velocity $(\omega_\alpha, \omega_\beta)$ must be real. Nayfeh proposed the computation of wave packet solutions determined by the six independent conditions: (i) the eigenvalue condition (4); (ii) $\text{Im } \omega_\alpha = \text{Im } \omega_\beta = 0$; (iii) $\text{Re } \omega$ fixed; (iv) $\text{Re } \beta$ fixed; and (v) $dx/dt = \omega_\alpha$, $dz/dt = \omega_\beta$. Under these conditions the N-factor is determined by

$$N = \int_{t_0}^t [-\omega_\alpha \text{Im}(\alpha) - \omega_\beta \text{Im}(\beta) + \text{Im}(\omega)] dt \quad (10)$$

Finally we study a modified non-conservative wave packet formulation in which α, β , and ω are determined by: (i) the eigenvalue condition (4); (ii) $\text{Im } \omega_\alpha = \text{Im } \omega_\beta = 0$; (iii) $\text{Re } \omega$ fixed with $\text{Im } \omega = 0$; and (iv) $dx/dt = \omega_\alpha$, $dz/dt = \omega_\beta$. The motivation for these latter conditions is simply that laminar flow over a LFC wing may be assumed steady so a wave packet should propagate at fixed real frequency. The N-factor is given by (10) with $\text{Im}(\omega) = 0$.

Calculations made with Nayfeh's formulation of the wave packet equations were extremely sensitive and gave transition prediction at highly variable and unpredictable values of the N factor. Therefore, we report in Sec. 4 only the results obtained by our modified wave packet formulation in which the condition $\text{Re } \beta$ fixed is dropped in favor of $\text{Im } \omega = 0$.

SECTION 3 - NUMERICAL METHOD

In the computer code SALLY¹, Eqs. (1) - (2) are solved using a spectral method based on Chebyshev polynomials⁵. The boundary layer direction y $0 \leq y < \infty$, is mapped into the finite interval $-1 \leq w < 1$ by the algebraic mapping

$$w = 2 \frac{y}{y+L} - 1 \quad (11)$$

and $\phi(y)$ is approximated as the finite Chebyshev polynomial series

$$\phi(y) = \sum_{n=0}^M a_n T_n(w) \quad (12)$$

The resulting algebraic eigenvalue problem is solved globally (if a guess for the eigenvalue is not available) by a generalized QR algorithm or locally (if a good guess is available) by inverse Rayleigh iteration⁶. The resulting scheme is very efficient and accurate.

Group velocity ($\vec{V}g = \frac{\partial \omega}{\partial \vec{k}}$) can be calculated using the adjoint eigenfunction of the Orr-Sommerfeld equation. Thus if the Orr-Sommerfeld equation is written as

$$L(\vec{k}, \vec{x}, \omega(\vec{k})) \phi = 0 \quad (13)$$

then the differentiation with respect to wave number k gives

$$\frac{\partial L}{\partial \vec{k}} \phi + \frac{\partial L}{\partial \omega} \frac{\partial \omega}{\partial \vec{k}} \phi + L \frac{\partial \phi}{\partial \vec{k}} = 0 \quad (14)$$

Taking the inner product of (14) with the adjoint η of the eigenfunction ϕ gives

$$\frac{\partial \omega}{\partial \vec{k}} = - \frac{(\eta, \frac{\partial L}{\partial \vec{k}} \phi)}{(\eta, \frac{\partial L}{\partial \omega} \phi)} \quad (15)$$

In order to correlate transition we calculate N-factor for a fixed real frequency and repeat the calculations for several other frequencies to find the most dangerous mode. The eigenvalue solver in SALLY¹ searches for the eigenvalue ω given α and β . So we iterate on $\text{Re } \alpha$, $\text{Im } \alpha$, $\text{Re } \beta$ and $\text{Im } \beta$ such that the conditions described above for modified wave packet method are satisfied. This is achieved usually in three iterations. Following equations are employed in this iterative process.

$$\begin{bmatrix} \text{Im } \omega_{\alpha\alpha} & \text{Re } \omega_{\alpha\alpha} & \text{Im } \omega_{\alpha\beta} & \text{Re } \omega_{\alpha\beta} \\ \text{Im } \omega_{\beta\alpha} & \text{Re } \omega_{\beta\alpha} & \text{Im } \omega_{\beta\beta} & \text{Re } \omega_{\beta\beta} \\ \text{Re } \omega_{\alpha} & -\text{Im } \omega_{\alpha} & \text{Re } \omega_{\beta} & -\text{Im } \omega_{\beta} \\ \text{Im } \omega_{\alpha} & \text{Re } \omega_{\alpha} & \text{Im } \omega_{\beta} & \text{Re } \omega_{\beta} \end{bmatrix} \begin{bmatrix} \text{Re } (\alpha - \alpha_0) \\ \text{Im } (\alpha - \alpha_0) \\ \text{Re } (\beta - \beta_0) \\ \text{Im } (\beta - \beta_0) \end{bmatrix} = \begin{bmatrix} -\text{Im } \omega_{\alpha} \\ -\text{Im } \omega_{\beta} \\ \text{Re } (\Omega - \omega) \\ -\text{Im } (\omega) \end{bmatrix} \quad (16)$$

The properties of the laminar boundary layer profiles required to solve (1) - (2) are obtained using a compressible boundary layer code for swept tapered wings developed by Kaups and Cebeci¹.

SECTION 4-
RESULTS

Burrows⁷ has reported flight transition data taken at Cranfield for a large, untapered, 45° swept half wing mounted as a dorsal fin upon the mid-upper fuselage of an Avro Lancaster airplane. The airfoil section was made-up of two semi-ellipses, one of which constituted a faired trailing edge and the other corresponding to the leading edge of a 10 percent thick airfoil, with effective chord of 10.83 feet, measured in the free stream direction. The location of the beginning of transition in the Cranfield data was estimated as given in Ref. 8. Two of the Cranfield flight tests were chosen for correlating transition using wave packet theory.

In the first test case, calculations were made for a chord Reynolds number of 11.7×10^6 and -2° angle of attack. In this flow, transition begins at $x/c = 5.5\%$. A maximum N factor of 7.6 was obtained at a frequency of 1250 Hz both with the envelope method and the modified wave packet method.

The predicted variation of the N factor up to the transition location was almost identical for the envelope method and the modified wave packet method. We also compute the solution of the conservative wave packet equations (6) - (9) in which only the real parts of equations (6) - (7) are taken while (8)-(9)

are solved in their full complex form. The resulting N factor at transition is 5.2. The variation of N factor with x/c for the various methods is plotted in Fig. 2.

Wave angle, wave length and the direction of the group velocity as predicted by the envelope and wave packet methods are given in Figs. 3 - 5. Although the results are qualitatively similar, there is appreciable quantitative difference in these parameters at the transition location. It is surprising that the N factor calculated by the envelope and modified wave packet methods are the same.

In the second test case, the angle of attack of the wing was changed to zero. In this case, transition occurred experimentally at $x/c = 7\%$. The envelope method gave an N factor of 10.8 at a frequency of 1000 Hz. The wave packet method gave a maximum N factor of 10.5 at a frequency of 1200 Hz, which is close to the prediction of the envelope method. The variation of N factor with x/c is plotted in Fig. 6. The predictions of the conservative wave packet approximation and a fixed wavelength, fixed frequency integration are also plotted in this figure. The conservative wave packet approximation gave an N factor at transition of 8.6 rather than 10.5.

Figure 7 shows the influence of frequency on N factor at transition for the wing as predicted by the wave packet theory. Wave angle, wave length and direction of the group velocity for this particular wing are shown in Figs. 8-10. Again there is substantial quantitative difference in the predictions of the two methods.

SECTION 5 - CONCLUSIONS

Calculations were made for a Cranfield 45° swept wing with $Re_c = 11.7 \times 10^6$ using a modified wave packet method and the envelope method. Both methods gave an N factor of 7.6 at transition location for an angle of attack, $\alpha_A = -2^\circ$. For $\alpha_A = 0^\circ$, the envelope and modified wave packet methods gave N factors of 10.8 and 10.5, respectively. Since it may be argued that the wave packet method is physically more relevant for predicting transition in three dimensional boundary layers, it was initially hoped that the wave packet method might give more consistent transition N factors. However, the results show that the wave packet method provides N factors which are at best as consistent as those of envelope method. Since the wave packet method is at least 3 times as expensive to use as the envelope method, the latter is recommended for engineering design calculations.

We would like to thank D. M. Bushnell and J. N. Hefner for helpful discussions. This work was supported by the National Aeronautics and Space Administration under Contract NAS1-15604.

REFERENCES

1. Srokowski, A. J., and Orszag, S. A., 'Mass Flow Requirements for LFC Wing Design', AIAA Paper No. 77-1222, 1977.
2. Nayfeh, A. H., 'Stability of Three-Dimensional Boundary Layers', AIAA Paper No. 79-0262, 1979.
3. Mack, L. M., 'Transition Prediction and Linear Stability Theory, In AGARD Conference Proceedings No. 224, Laminar-Turbulent Transitions, Paper No. 1, 1977.
4. Courant, R. and Hilbert, D., Methods of Mathematical Physics, Vol.2, Interscience Publishing Co., New York, 1962.
5. Orszag, S. A., 'Accurate Solution of the Orr-Sommerfeld Equation', Journal of Fluid Mechanics, Vol. 50, 1971, p. 689.
6. Benney, D. J. and Orszag, S. A., 'Stability Analysis for Laminar Flow Control', NASA CR-2910, 1977.
7. Burrows, F. M., 'A Theoretical and Experimental Study of the Boundary Layer Flow on a 45° Swept Back Wing', COA Report No. 109, The College of Aeronautics, Cranfield, 1956.
8. Hefner, J. N. and Bushnell, D. M., Application of Stability Theory to Laminar Flow Control', Paper presented at the 12th AIAA Fluid and Plasma Dynamics Conference, July 24-26, 1979, Williamsburg, Virginia.

FIGURE CAPTIONS

Figure 1. A plot of the coordinate system on a swept wing.

Figure 2. A plot of N versus percent of chord x/c for various methods applied to a swept wing of an Avro Lancaster airplane at -2° angle of attack. Solid curve: modified wave packet method and envelope method at $f = 1250$ Hz which gives nearly the maximum N at the transition point. Dashed curve: result of integrating equations (6) - (9) across the wing with (6) and (7) replaced by their real parts. The curves are plotted from the beginning of the unstable flow region until the transition point at $x/c = 5.5\%$.

Figure 3. A plot of wave propagation angle versus x/c for the same flow as in Figure 2.

Figure 4. A plot of wavelength versus x/c for the same flow as in Figure 2.

Figure 5. A plot of the direction of the group velocity for the same flow as in Figure 2.

Figure 6. Same as Fig. 2 except for the wing at 0° angle of attack. In addition to the results of the wave packet methods and envelope method, the N

factor obtained by integrating a fixed wavelength, fixed frequency mode across the wing is given. Here N is given by (5) and the mode is determined by the six real conditions: (i) $F = (4)$; (ii) $\text{Im } \alpha = -\text{Im } \beta = 0$; (iii) $\lambda/c = 0.001$; (iv) $\text{Re } \omega = 750 \text{ Hz}$.

Figure 7. Variation of N at transition versus frequency obtained using the modified wave packet method for the same flow as in Figure 6.

Figure 8. A plot of wave propagation angle versus x/c for the same flow as in Figure 6.

Figure 9. A plot of wavelength versus x/c for the same flow as in Figure 6.

Figure 10. A plot of the direction of the group velocity for the same flow as in Figure 6.

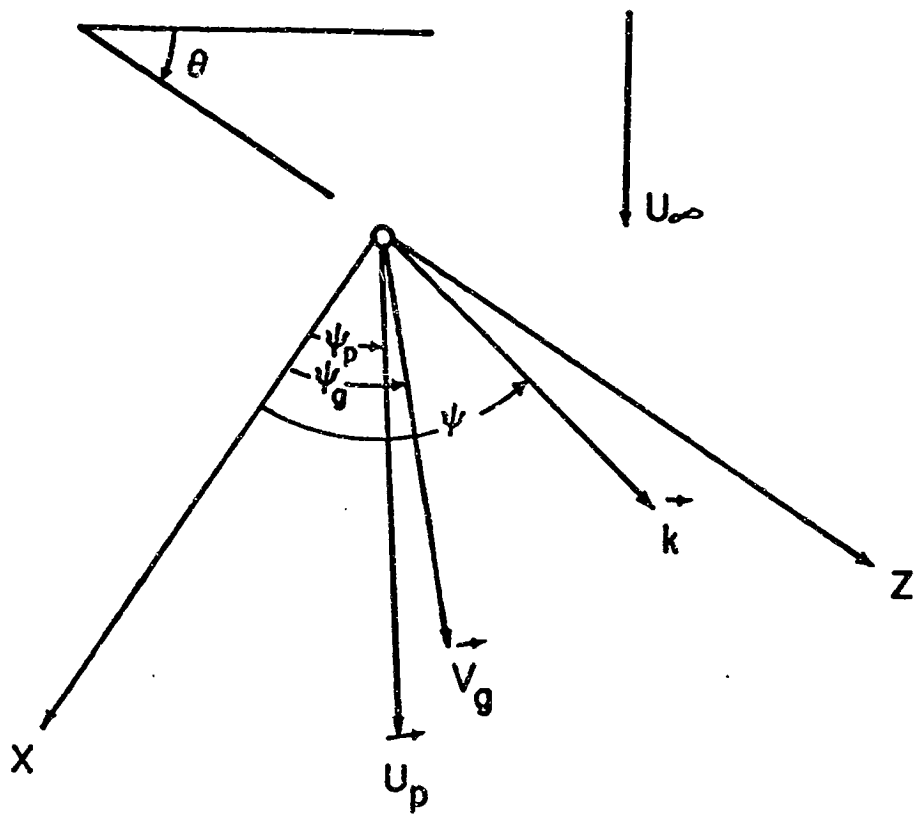


Figure 1.

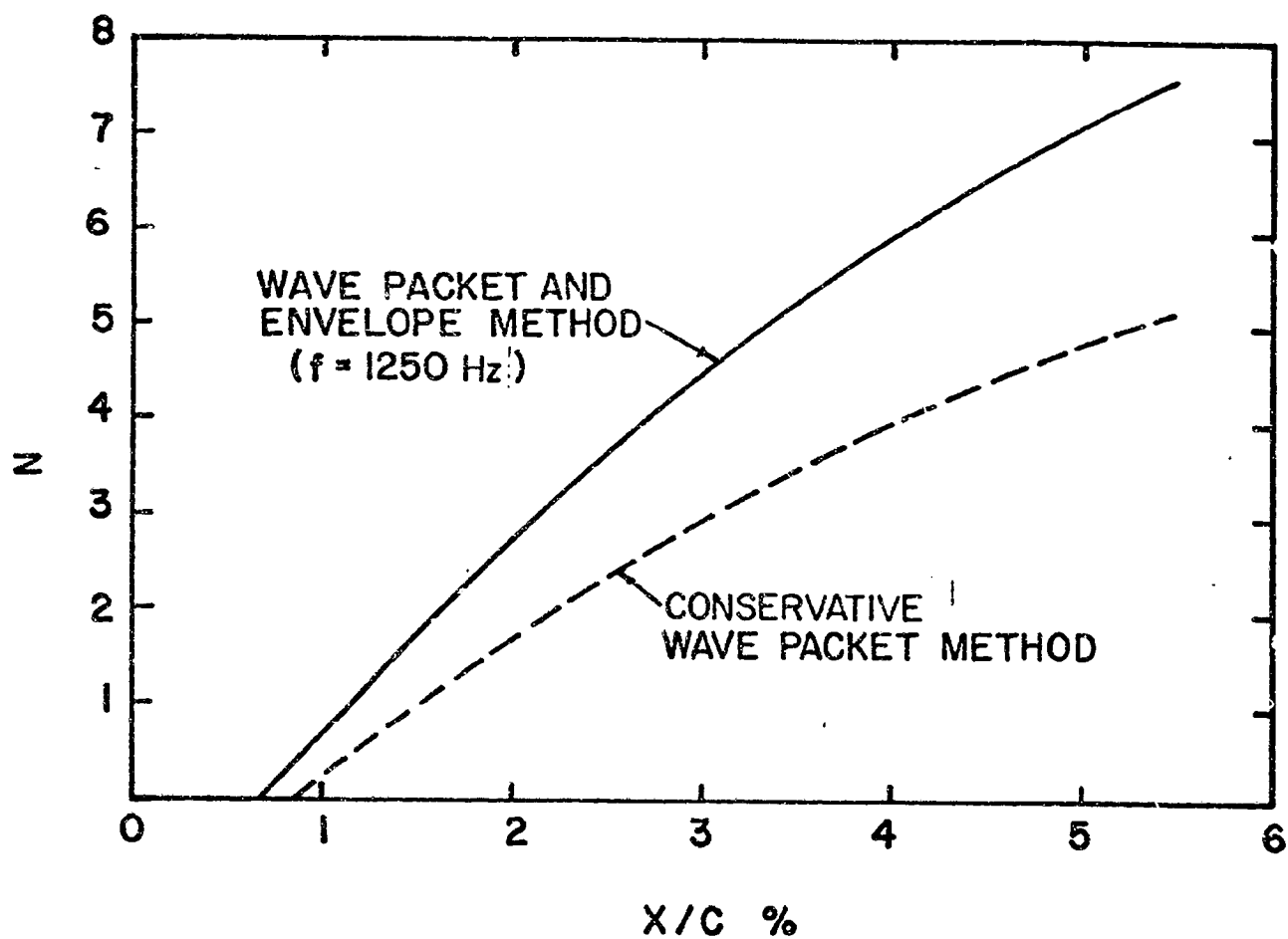


Figure 2.

ORIGINAL PAGE IS
OF POOR QUALITY

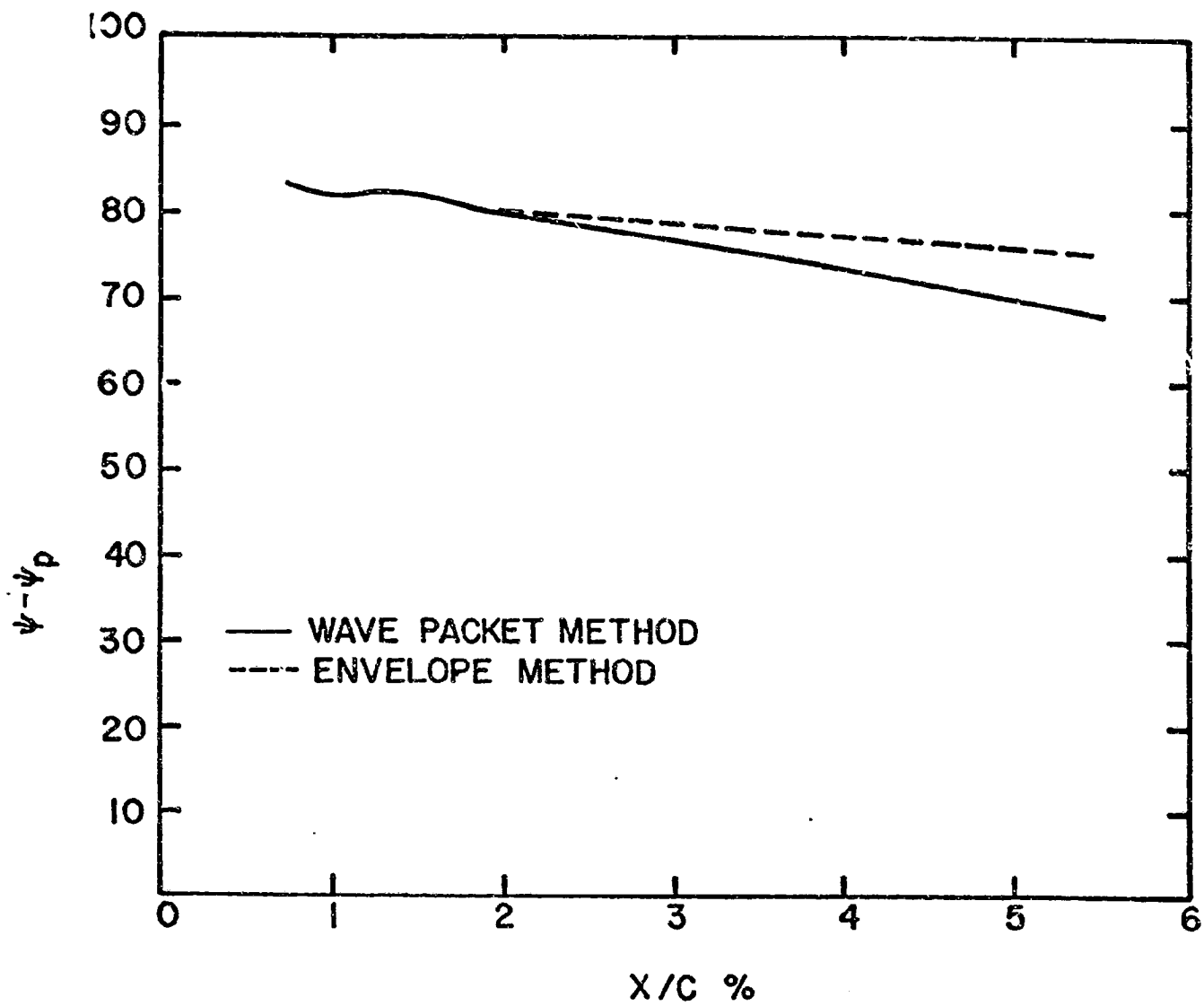


Figure 3.

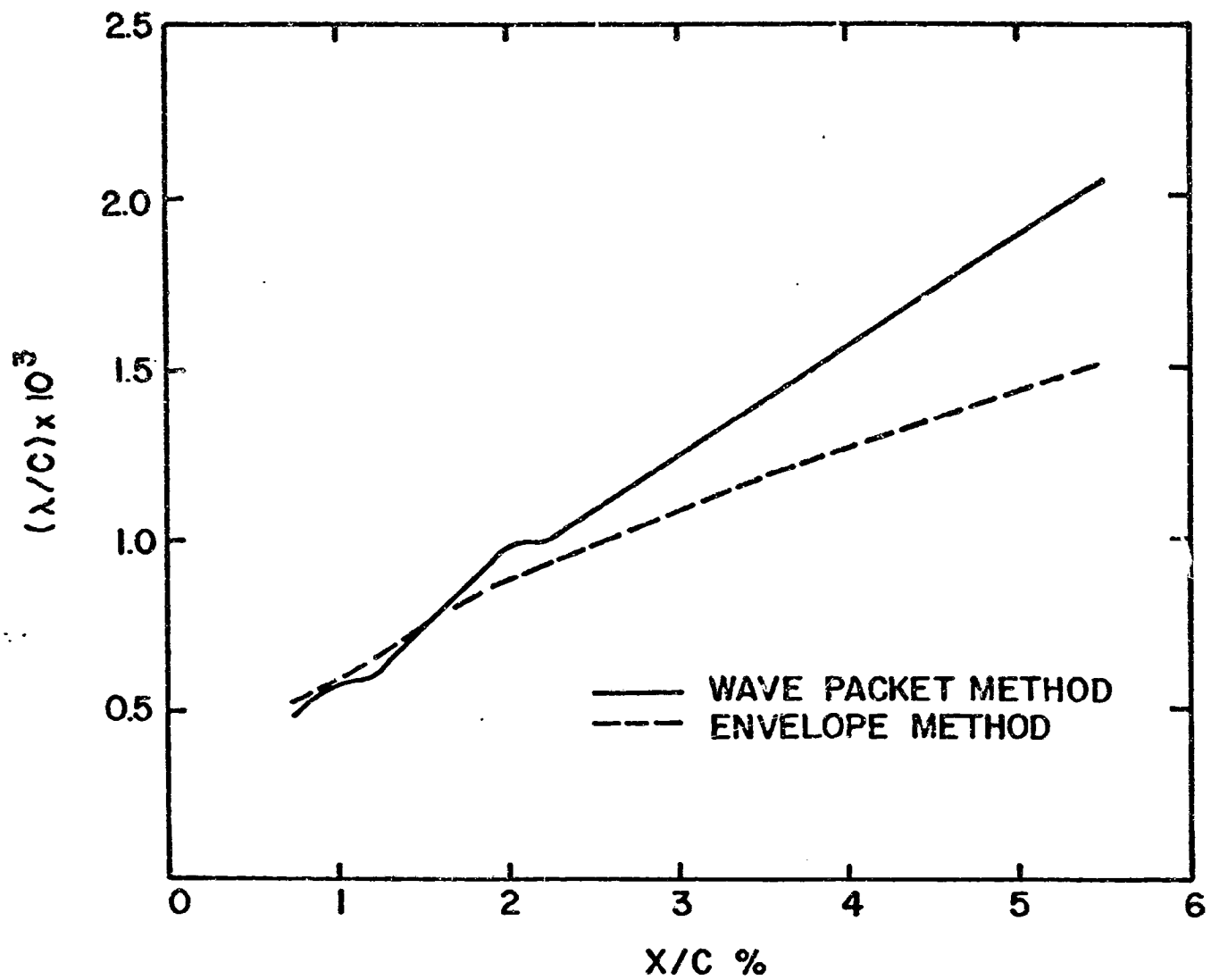


Figure 4

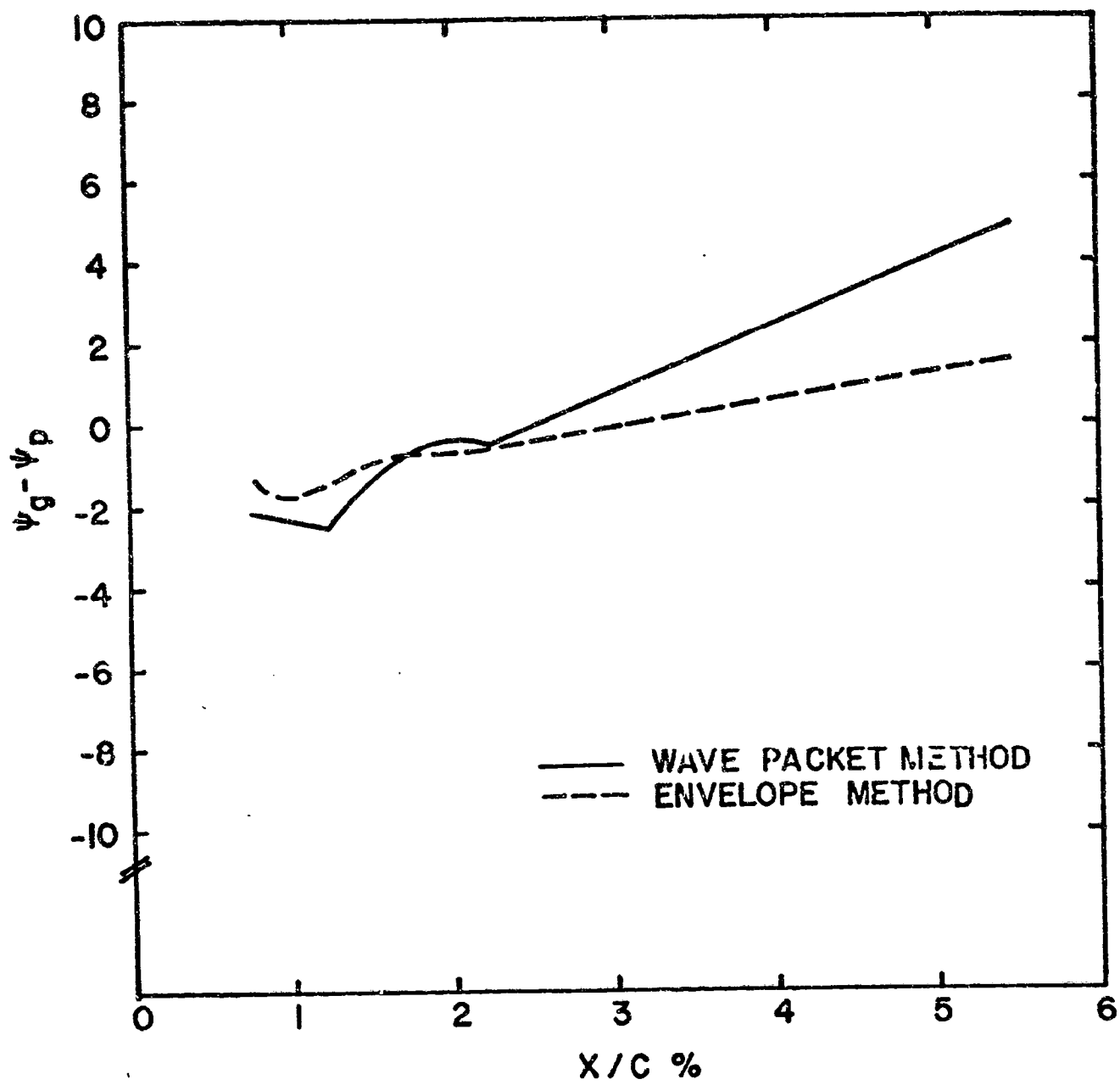


Figure 5.

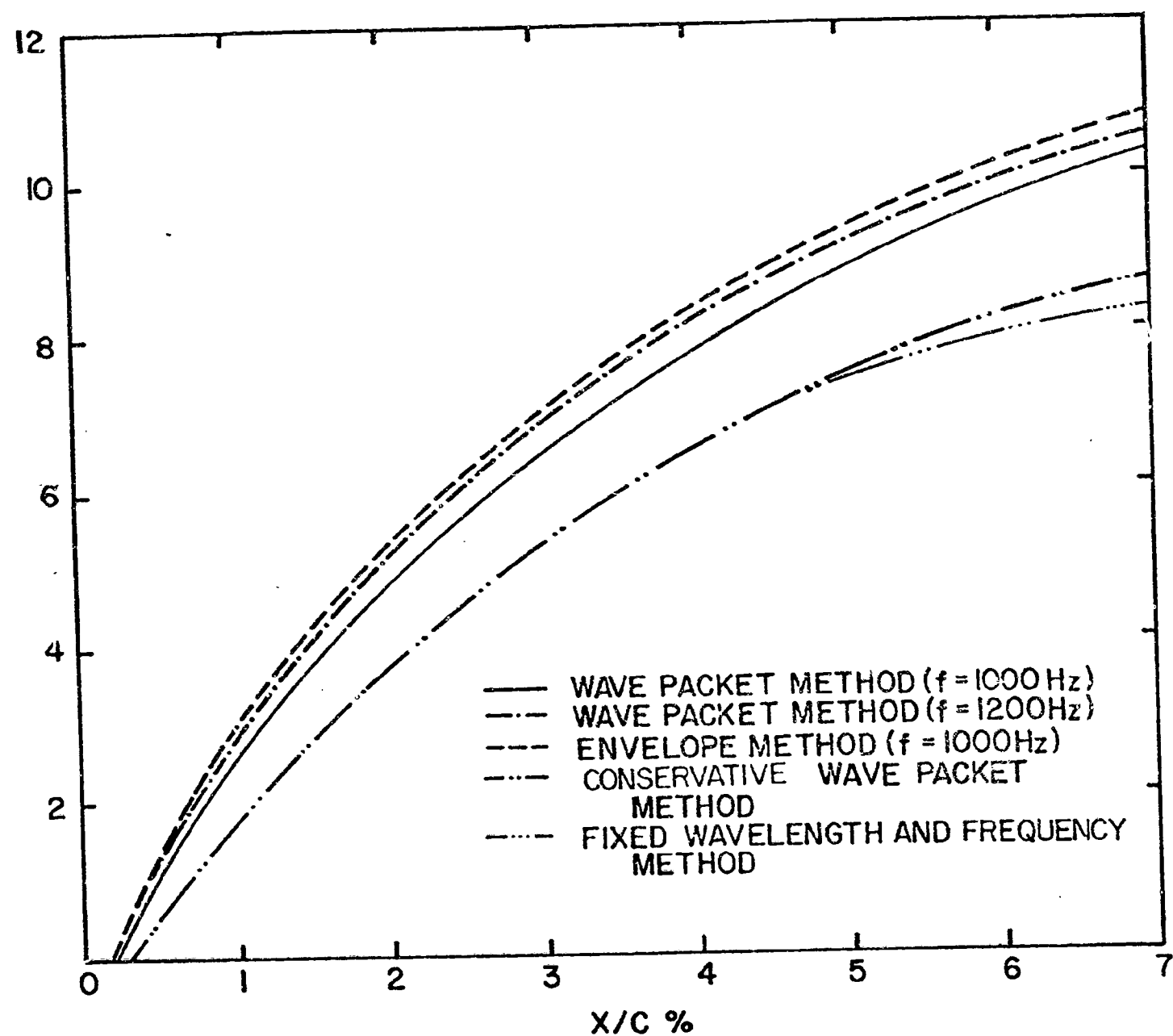


Figure 6.

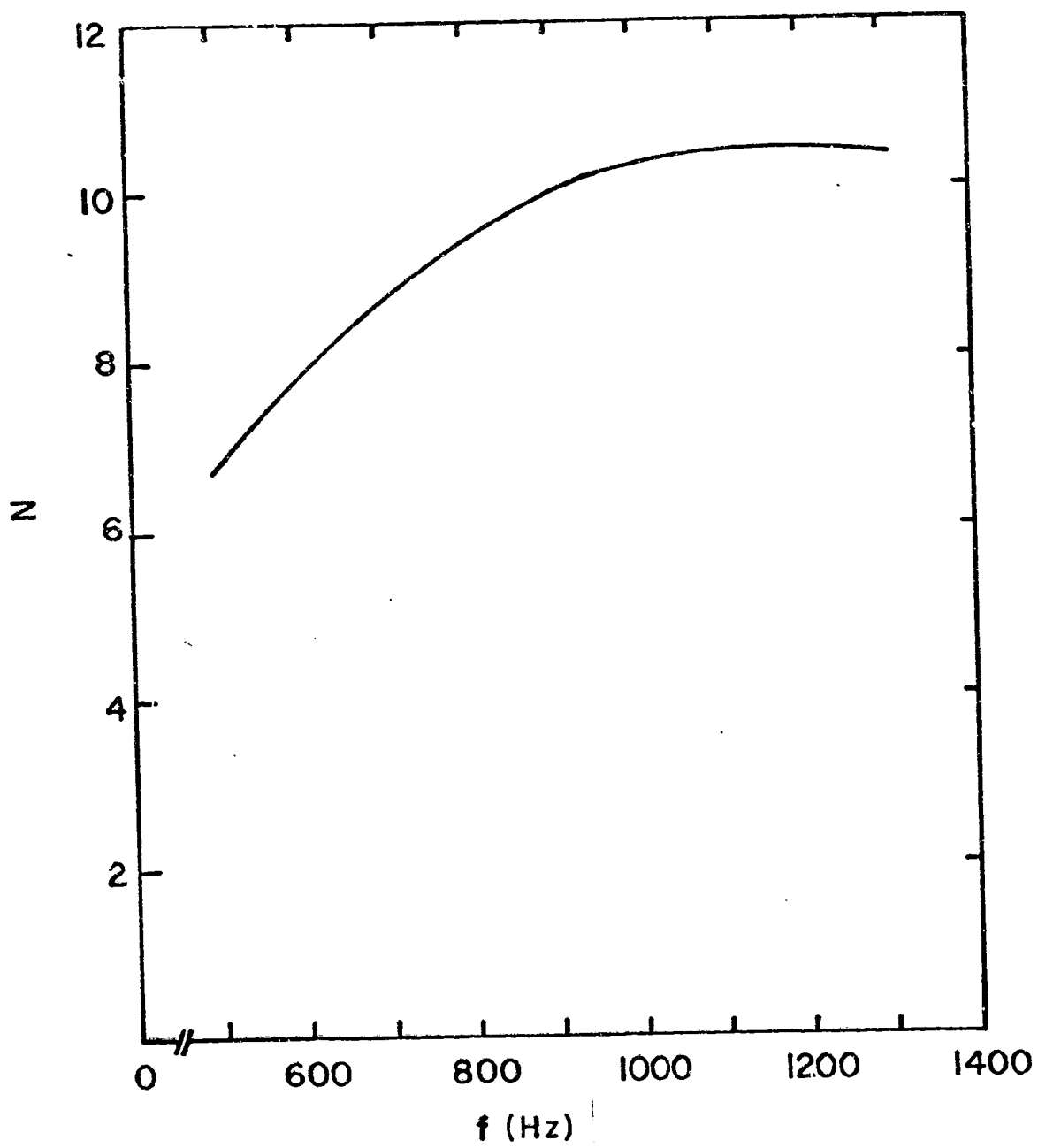


Figure 7.

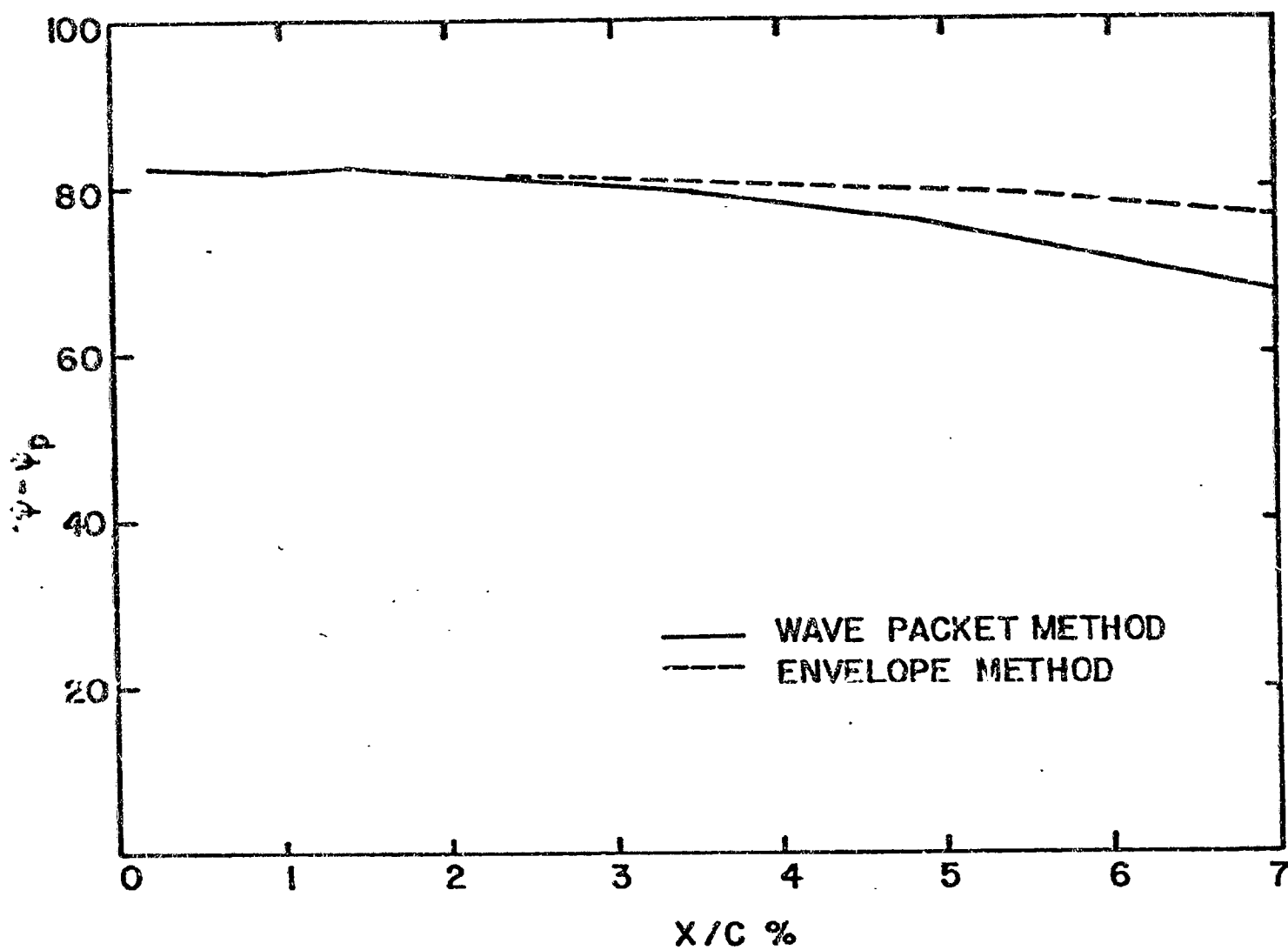


Figure 8.

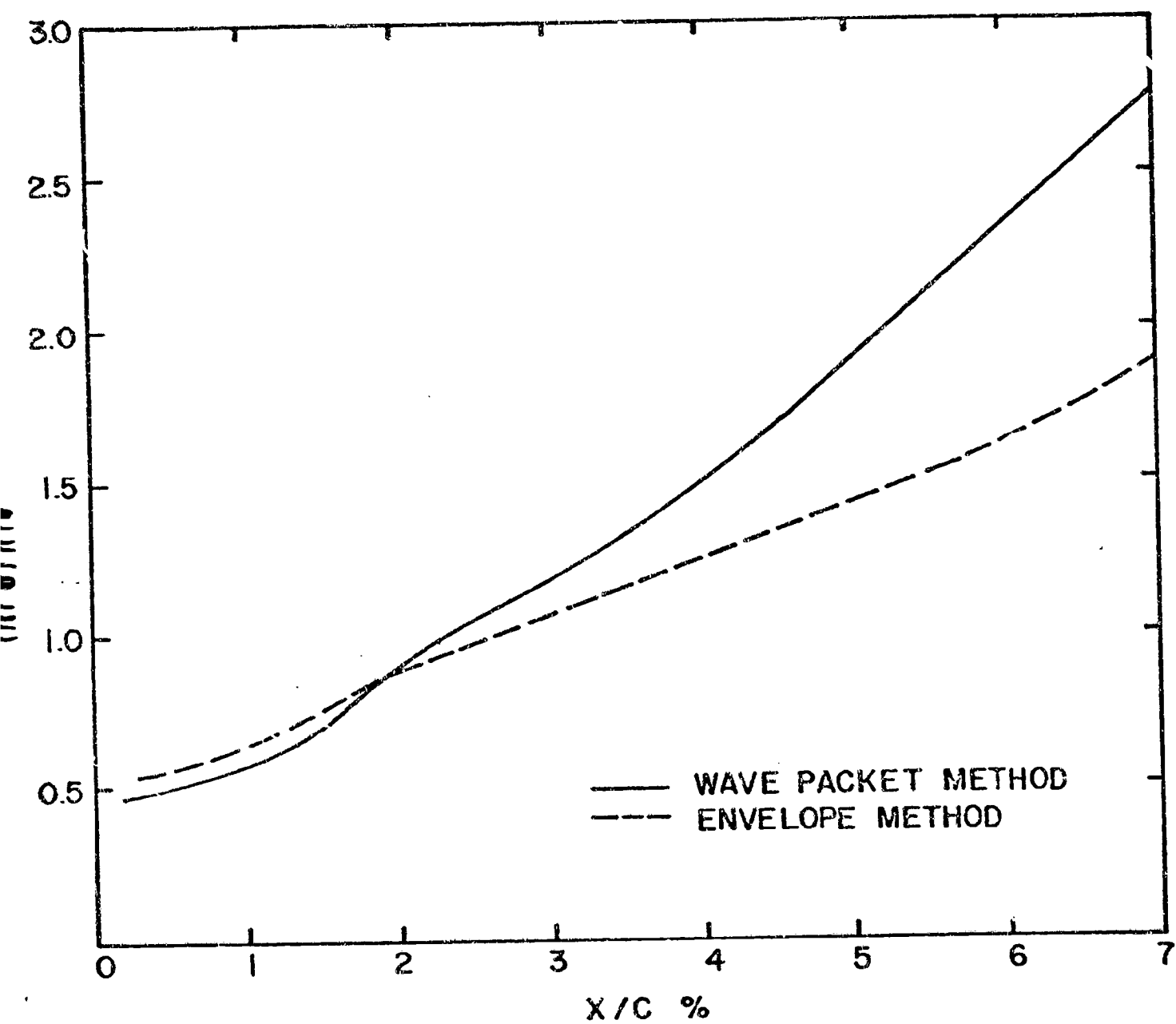


Figure 9.

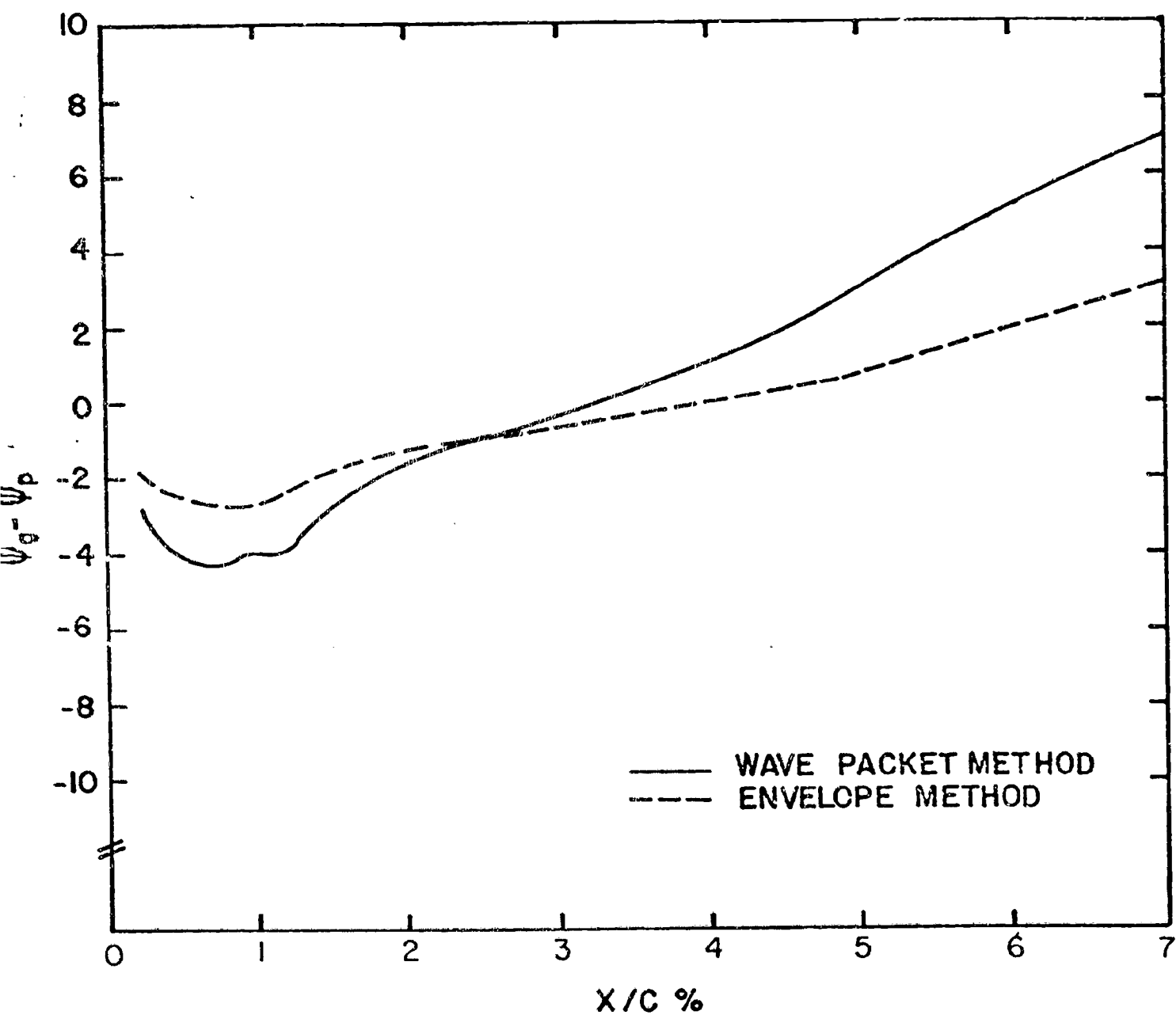


Figure 10.